

Lattice quark propagator with staggered quarks in Landau and Laplacian gauges

Patrick O. Bowman and Urs M. Heller

Department of Physics and School for Computational Science and Information Technology, Florida State University, Tallahassee, Florida 32306-4120

Anthony G. Williams

Special Research Centre for the Subatomic Structure of Matter and The Department of Physics and Mathematical Physics, Adelaide University, 5005, Australia

(Received 6 March 2002; published 30 July 2002)

We report on the lattice quark propagator using standard and improved staggered quark actions, with the standard Wilson gauge action. The standard Kogut-Susskind action has errors of $\mathcal{O}(a^2)$ while the ‘‘Asqtad’’ action has $\mathcal{O}(a^4)$, $\mathcal{O}(a^2g^2)$ errors. The quark propagator is interesting for studying the phenomenon of dynamical chiral symmetry breaking and as a testbed for improvement. Gauge dependent quantities from lattice simulations may be affected by Gribov copies. We explore this by studying the quark propagator in both Landau and Laplacian gauges. Landau and Laplacian gauges are found to produce very similar results for the quark propagator.

DOI: 10.1103/PhysRevD.66.014505

PACS number(s): 12.38.Gc, 11.15.Ha, 12.38.Aw, 14.65.-q

I. INTRODUCTION

The quark propagator lies at the heart of most QCD physics. In the low momentum region it exhibits dynamical chiral symmetry breaking (which cannot be seen from perturbation theory) and at high momentum can be used to extract the running quark mass [1,2] (which cannot be extracted directly from experiment). In lattice QCD, quark propagators are tied together to extract hadron masses. Lattice gauge theory provides a way to study the quark propagator nonperturbatively, possibly as a way of calculating the chiral condensate and Λ_{QCD} , and in turn, such a study can provide technical insight into lattice gauge theory.

We study the quark propagator using the Kogut-Susskind (KS) fermion action, which has $\mathcal{O}(a^2)$ errors, and an improved staggered action, Asqtad [3], which has errors of $\mathcal{O}(a^4)$, $\mathcal{O}(a^2g^2)$. These choices complement other studies using clover [4,5] and overlap [6] quarks. We are required to gauge fix and we choose the ever popular Landau gauge and the interesting Laplacian gauge [7,8]. Laplacian gauge fixing is an unambiguous gauge fixing and, although it is difficult to understand perturbatively, it is equivalent to the Landau gauge in the asymptotic region. It has been used to study the gluon propagator [9–11].

In $SU(N)$ there are various ways to implement a Laplacian gauge fixing. Three varieties of Laplacian gauge fixing are used, and these form three different, but related gauges. This is briefly discussed in Sec. III. For a more detailed discussion, see Ref. [11].

The quark propagator was calculated on 80, $16^3 \times 32$ configurations generated with the standard Wilson gluon action at $\beta = 5.85$ ($a = 0.130$ fm) [12]. We have used six quark masses: $am = 0.075, 0.0625, 0.05, 0.0375, 0.025, \text{ and } 0.0125$ (114–19 MeV).

II. LATTICE QUARK PROPAGATOR

In the continuum, Lorentz invariance allows us to decompose the full propagator into Dirac vector and scalar pieces

$$S^{-1}(p^2) = iA(p^2)\gamma \cdot p + B(p^2) \quad (1)$$

or, alternatively,

$$S^{-1}(p^2) = Z^{-1}(p^2)[i\gamma \cdot p + M(p^2)]. \quad (2)$$

This is the bare propagator which, once regularized, is related to the renormalized propagator through the renormalization constant

$$S(a; p^2) = Z_2(a; \mu)S^{\text{ren}}(\mu; p^2), \quad (3)$$

where a is some regularization parameter, e.g., lattice spacing. Asymptotic freedom implies that, as $p^2 \rightarrow \infty$, $S(p^2)$ reduces to the free propagator

$$S^{-1}(p^2) \rightarrow i\gamma \cdot p + m_0, \quad (4)$$

where m_0 is the bare quark mass.

The tadpole improved, tree-level form of the KS quark propagator is

$$S_{\alpha\beta}^{-1}(p; m) = u_0 i \sum_{\mu} (\bar{\gamma}_{\mu})_{\alpha\beta} \sin(p_{\mu}) + m \bar{\delta}_{\alpha\beta}, \quad (5)$$

where p_{μ} is the discrete lattice momentum given by

$$p_{\mu} = \frac{2\pi n_{\mu}}{aL_{\mu}}, \quad n_{\mu} \in \left[\frac{-L_{\mu}}{4}, \frac{L_{\mu}}{4} \right]. \quad (6)$$

For the tadpole factor, we employ the plaquette measure,

$$u_0 = \left(\frac{1}{3} \text{Re Tr} \langle P_{\mu\nu} \rangle \right)^{1/4}. \quad (7)$$

We give a detailed discussion of the notation used for the staggered quark actions in the Appendix. As a convenient short-hand we define a new momentum variable for the KS quark propagator:

$$q_\mu \equiv \sin(p_\mu). \quad (8)$$

We can then decompose the inverse propagator [14]

$$Z^{-1}(q) = \frac{1}{16N_c i q^2} \text{Tr} \{ \bar{\gamma} \cdot q S^{-1} \}, \quad (9)$$

$$M(q) = \frac{1}{16N_c} \text{Tr} \{ S^{-1} \}, \quad (10)$$

where the factor of 16 comes from the trace over the spin-flavor indices of the staggered quarks and N_c from the trace over color. Comparing Eqs. (4) and (5) we see that dividing out q^2 in Eq. (9) is analogous to dividing out p^2 in the continuum and ensures that Z has the correct asymptotic behavior. So by considering the propagator as a function of q_μ , we ensure that the lattice quark propagator has the correct tree-level form, i.e.,

$$S^{\text{tree}}(q_\mu) = \frac{1}{i \bar{\gamma} \cdot q + m}, \quad (11)$$

and hopefully better approximates its continuum behavior. This is the same philosophy that has been used in studies of the gluon propagator [15] and Eq. (8) was used to define the momentum in Ref. [2].

The Asqtad quark action [3] is a fat-link Staggered action using three-link, five-link, and seven-link staples to minimize flavor changing interactions along with the three-link Naik term [16] (to correct the dispersion relation) and planar five-link Lepage term [17] (to correct the IR). The coefficients are tadpole improved and tuned to remove all tree-level $\mathcal{O}(a^2)$ errors. This action was motivated by the desire to improve flavor symmetry, but has also been reported to have good rotational properties.

The quark propagator with this action has the tree-level form

$$S_{\alpha\beta}^{-1}(p; m) = u_0 i \sum_{\mu} (\bar{\gamma}_{\mu})_{\alpha\beta} \sin(p_{\mu}) [1 + \frac{1}{6} \sin^2(p_{\mu})] + m \bar{\delta}_{\alpha\beta}, \quad (12)$$

so we repeat the above analysis, this time defining

$$q_\mu \equiv \sin(p_\mu) [1 + \frac{1}{6} \sin^2(p_\mu)]. \quad (13)$$

Finally, it should be noted that both actions get contributions from tadpoles, which can be seen in the tree-level behaviors of the two invariants

$$Z^{\text{tree}} = \frac{1}{u_0}, \quad (14)$$

$$M^{\text{tree}} = \frac{m_0}{u_0}, \quad (15)$$

so inserting the tadpole factors provides the correct normalization.

III. GAUGE FIXING

We consider the quark propagator in Landau and Laplacian gauges. Landau gauge fixing is performed by enforcing the Lorentz gauge condition, $\sum_{\mu} \partial_{\mu} A_{\mu}(x) = 0$ on a configuration by configuration basis. This is achieved by maximizing the functional,

$$\mathcal{F} = \frac{1}{2} \sum_{x, \mu} \text{Tr} \{ U_{\mu}(x) + U_{\mu}^{\dagger}(x) \}, \quad (16)$$

by, in this case, a Fourier accelerated, steepest-descent algorithm [18]. There are, in general, many such maxima and these are called lattice Gribov copies. While this ambiguity has produced no identified artifacts in QCD, in principle it remains a source of uncontrolled systematic error.

The Laplacian gauge is a nonlinear gauge fixing that respects rotational invariance, has been seen to be smooth, yet is free of Gribov ambiguity. It is also computationally cheaper than the Landau gauge. There is, however, more than one way of obtaining such a gauge fixing in $SU(N)$. The three implementations of Laplacian gauge fixing employed here are (in our notation):

(1) ∂^2 (I) gauge (QR decomposition), used by Alexandrou *et al.* [9];

(2) ∂^2 (II) gauge, where the Laplacian gauge transformation is projected onto $SU(3)$ by maximizing its trace [11]; and

(3) ∂^2 (III) gauge (Polar decomposition), the original prescription described in Ref. [7] and tested in Ref. [8].

All three versions reduce to the same gauge in $SU(2)$. For a more detailed discussion, see Ref. [11].

IV. ANALYSIS OF LATTICE ARTIFACTS

A. Tree-level correction

As mentioned above, the idea of a “kinematic” or “tree-level” correction has been used widely in studies of the gluon propagator [15] and the quark propagator [4–6] and we investigate its application to our quark propagators. For the moment we shall restrict ourselves to the Landau gauge. To help us understand the lattice artifacts, we separate the data into momenta lying entirely on a spatial Cartesian direction (squares), along the temporal direction (triangles), the four-diagonal (diamonds), or some other combination of directions (circles).

The Z function is plotted for the KS action in Fig. 1, comparing the results using p and q . In the top of Fig. 1 we see substantial hypercubic artifacts (in particular look at the difference between the diamond and the triangle at around 2.5 GeV). We can suggest that this is caused by the violation of rotational symmetry because the agreement between triangles and squares suggests that finite volume effects are small in the region of interest. In the plot below, where q has been used, we see some restoration of rotational symmetry.

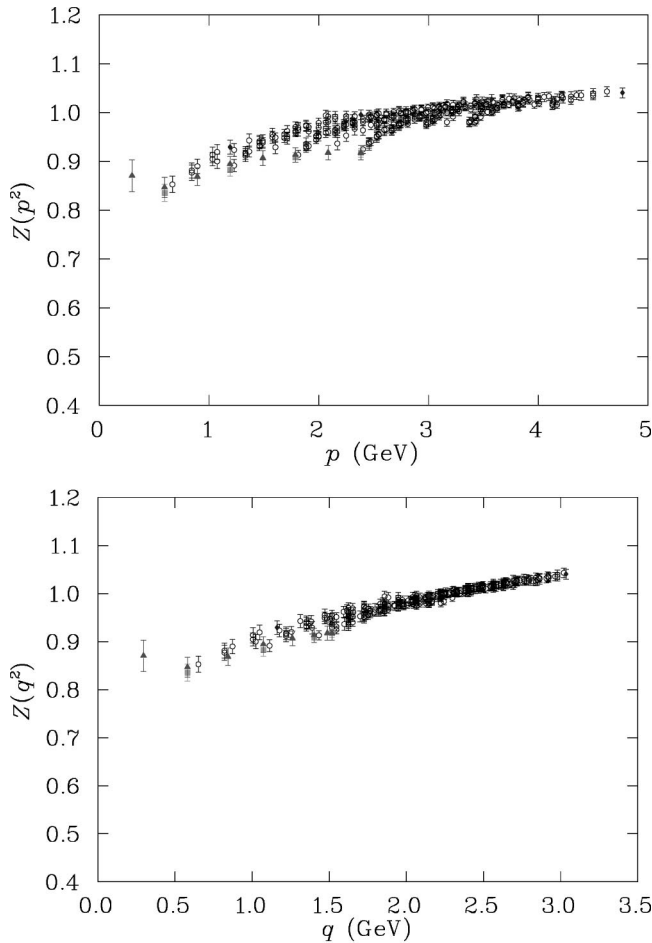


FIG. 1. Z function for quark mass $ma=0.05$ ($m\approx 76$ MeV) for the KS action in the Landau gauge. The top figure is plotted using the standard lattice momentum p and the bottom uses the “action” momentum q . Note that this choice affects only the horizontal scale.

The same study is made for the Asqtad action in Fig. 2. In both cases this action shows a substantial improvement over the KS action, and when we plot using q , the momentum defined by the action, rotational asymmetry is reduced to the level of the statistical errors.

It is less clear which momentum variable should be used for the mass function, so for consistency we use q , as for the Z function. The effect of this is shown in Fig. 3. For ease of comparison, both sets of data have been cylinder cut [15]. In the case of the mass function, the choice of momentum will actually make little difference to our results.

B. Comparison of the actions

In Fig. 4 the mass function is plotted, in the Landau gauge, for both actions with a quark mass $ma=0.05$. This time there have been no data cuts. We see that the KS action gives a much larger value for $M(0)$ than the Asqtad action and is slower to approach asymptotic behavior. Asqtad also shows slightly better rotational symmetry.

Looking back at Figs. 1 and 2 we see that the Asqtad action displays clearly better rotational symmetry in the

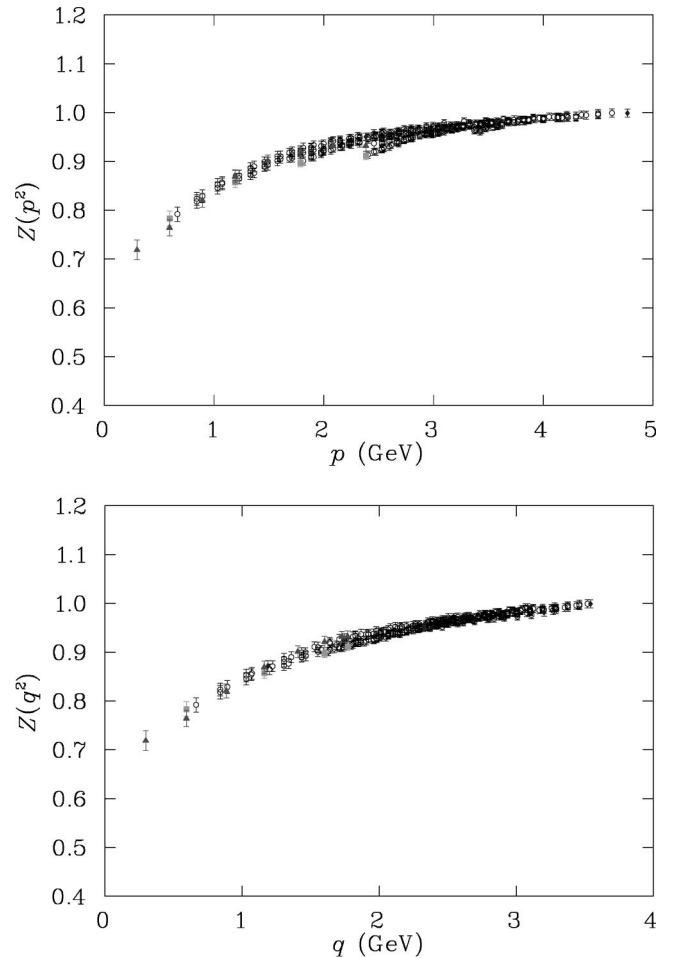


FIG. 2. Z function for quark mass $ma=0.05$ ($m\approx 76$ MeV) for the Asqtad action in the Landau gauge. The top figure is plotted using the standard lattice momentum p and the bottom uses the “action” momentum q .

quark Z function and, curiously, improved infrared behavior as well. The Asqtad action also displays a better approach to asymptotic behavior, approaching one in the ultraviolet. The relative improvement increases as the quark mass decreases. In Fig. 5 we compare the mass function for the two actions at $ma=0.0125$, the lowest mass studied here. The low quark mass has introduced less noise into the propagator with the Asqtad action than with the KS action.

C. Comparative performance of Landau and Laplacian gauges

Figure 6 shows the mass function for the Asqtad action in $\partial^2(\text{I})$ and $\partial^2(\text{II})$ gauges and it should be compared with the equivalent Landau gauge result in Fig. 4 (bottom). We see first that these three gauges give very similar results (we shall investigate this in more detail later) and second that they give similar performance in terms of rotational symmetry and statistical noise. Looking more closely, we can see that the Landau gauge gives a slightly cleaner signal at this lattice spacing.

The Landau gauge seems to respond somewhat better than the $\partial^2(\text{II})$ gauge to vanishing quark mass; compare Fig. 7

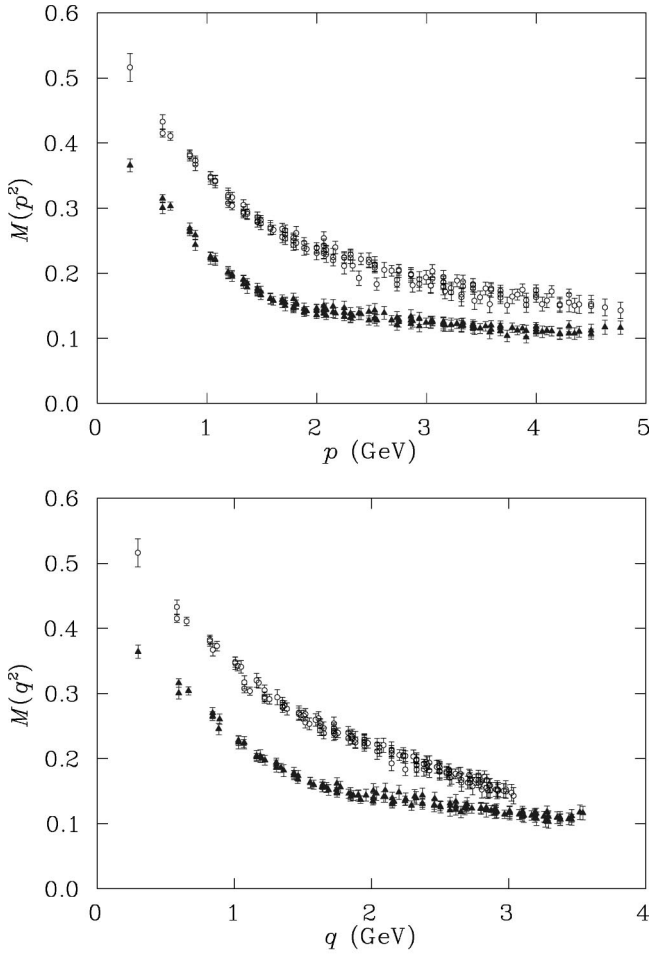


FIG. 3. The quark mass function for quark mass $ma = 0.05$ ($m \approx 76$ MeV) for the KS action (open circles) and the Asqtad action (solid triangles) in the Landau gauge. The top figure is plotted using the standard lattice momentum, and the bottom using the “action” momentum.

with Fig. 5 (bottom). In Fig. 7 we see large errors in the infrared region and points along the temporal axis lying below the bulk of the data. These are indicators of finite volume effects, an unexpected result given that earlier gluon propagator studies [9,10] appear to conclude that the Laplacian gauge is less sensitive to volume than the Landau gauge.

$\partial^2(\text{III})$ performs very poorly: see Fig. 8. The gauge fixing procedure failed for four of the configurations and eight of the remaining configurations produced Z and M functions with pathological negative values. Removing the negative contributions from the sample removed much of the noise, but the results were still poor. We have seen that this type of gauge fixing fails to produce a gluon propagator that has the correct asymptotic behavior [11]. The problem is that occasionally we encounter matrices with vanishing determinants which are destroying the projection onto $SU(3)$. We expect the degree to which this problem occurs to be dependent on the simulation parameters and the numerical precision used (in this work the gauge transformations were calculated in single precision).

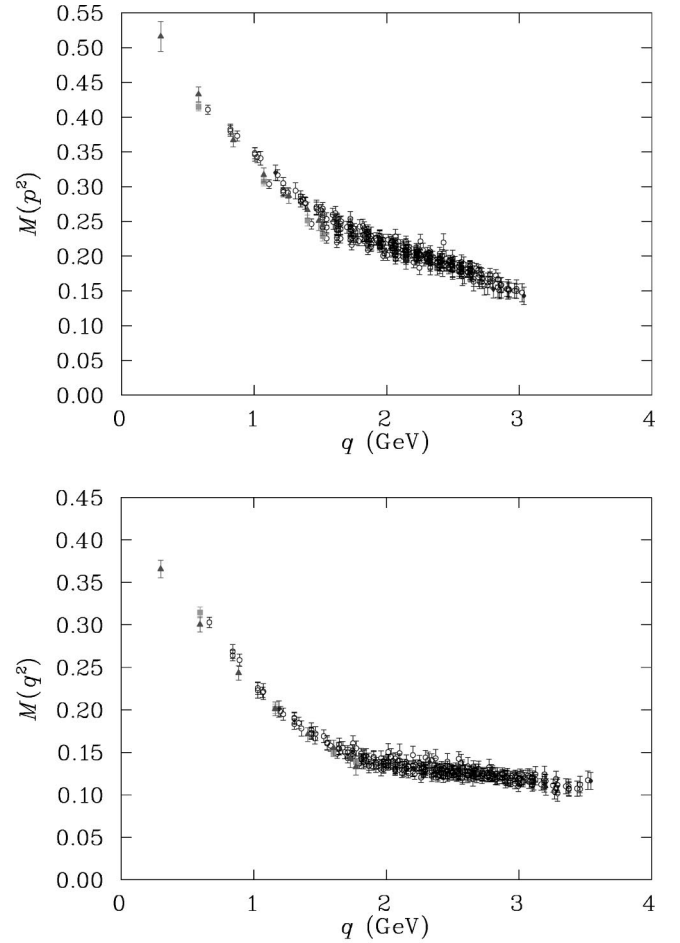


FIG. 4. Mass function for quark mass $ma = 0.05$ ($m \approx 76$ MeV), KS action (top), and Asqtad action (bottom) in the Landau gauge.

V. GAUGE DEPENDENCE

Now we investigate the quark mass and Z functions in Landau, $\partial^2(\text{I})$, and $\partial^2(\text{II})$ gauges. Figure 9 shows the Z function for the Asqtad action in Landau, $\partial^2(\text{I})$, and $\partial^2(\text{II})$ gauges. All three are in excellent agreement in the ultraviolet—as they should—but in the Laplacian gauges Z differs significantly from Z in the Landau gauge, in the infrared. The Z function in the Laplacian gauges is more strongly infrared suppressed than in the Landau gauge. There may be a small difference in $Z(q^2)$ between $\partial^2(\text{I})$ and $\partial^2(\text{II})$ gauges.

In all cases the quark Z function demonstrates little mass dependence. Deviation of Z from its asymptotic value of 1 is a sign of dynamical symmetry breaking, so we expect the infrared suppression to go away in the limit of an infinitely heavy quark. In Fig. 10 we show the Z function in the Landau gauge for the lightest and the heaviest quark masses in this study. The two are the same, to within errors, although if we look at the lowest momentum data we see that the point for the low mass lies below the high mass one. Figure 11 shows Z in the $\partial^2(\text{II})$ gauge for three quark masses. Again, the data are consistent, to within errors, but there is a sys-

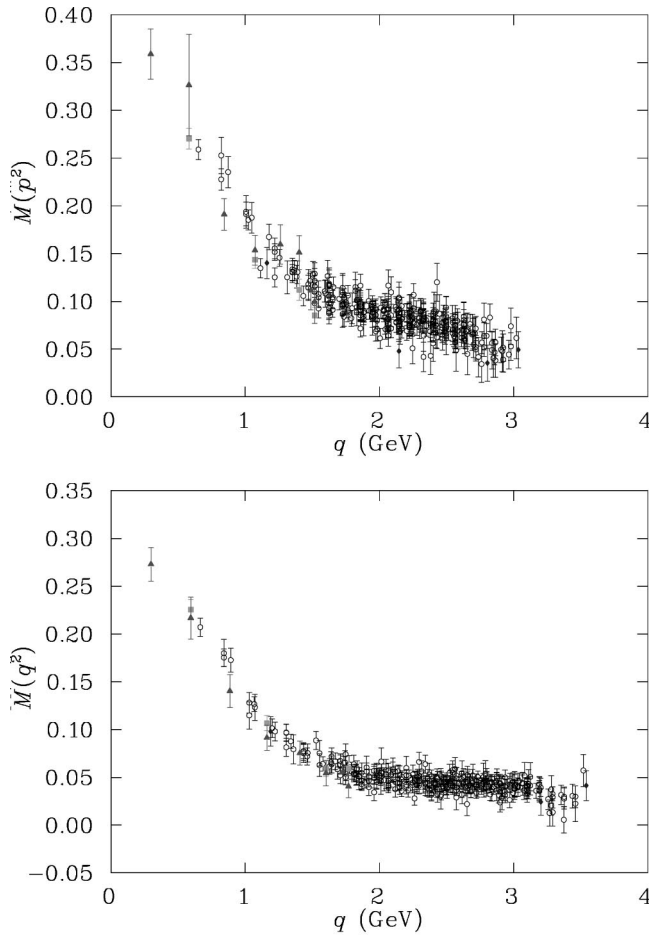


FIG. 5. Mass function for quark mass $ma=0.0125$ ($m \simeq 19$ MeV), KS action (top), and Asqtad action (bottom) in the Landau gauge. In both cases, lowering the quark mass increases the amount of noise, but the Asqtad action seems to be affected less than the KS action. Note that the y axis for the bottom figure starts below zero.

tematic ordering of lightest to heaviest. We conclude from this that behavior is consistent with expectations, dependence on the quark mass, if any, is very weak. One possible explanation is that all the masses studied are light, less than or approximately equal to the strange quark mass, and that heavier masses will affect the Z function more clearly.

The mass functions in Landau and ∂^2 (I) gauges, shown in Fig. 12, agree to within errors. The data for the ∂^2 (I) gauge seems to sit a little higher than the Landau gauge through most of the momentum range, so with greater statistics we may resolve a small difference. The mass functions are nearly identical in ∂^2 (I) and ∂^2 (II) gauges: see Fig. 13.

VI. MODELING THE MASS FUNCTION

The Asqtad quark mass function at each value of the mass has been cylinder cut and extrapolated—by a quadratic fit at each momentum—to zero mass. The quadratic fit was chosen on purely practical grounds and a linear fit worked almost as

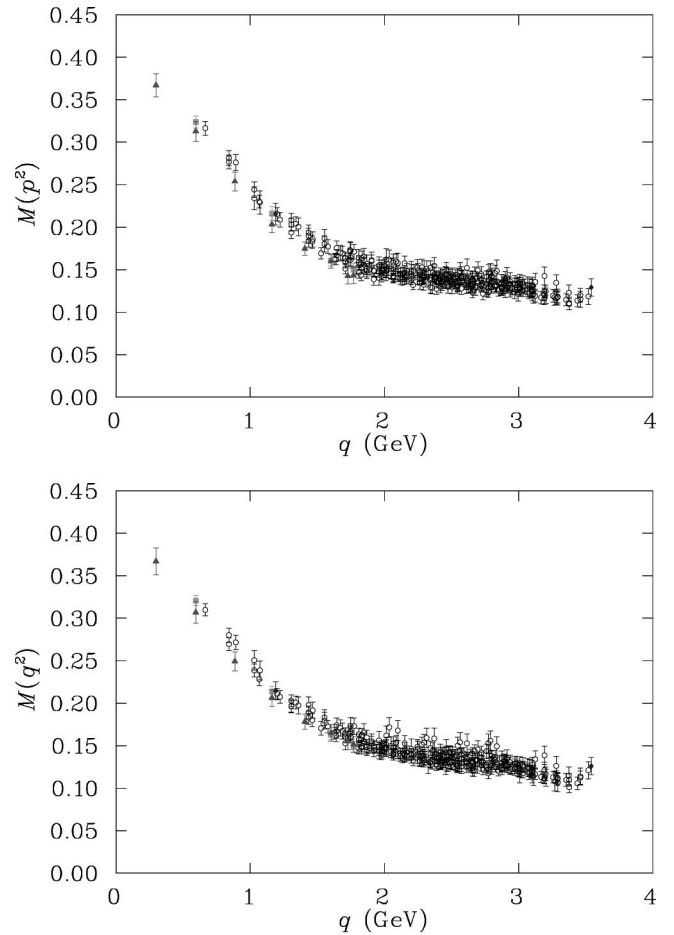


FIG. 6. Mass function for quark mass $ma=0.05$ ($m \simeq 76$ MeV), Asqtad action in the ∂^2 (I) and ∂^2 (II) gauges. Comparing with Fig. 4 (bottom) we see that the Landau, ∂^2 (I) and ∂^2 (II), gauges yield similar results.

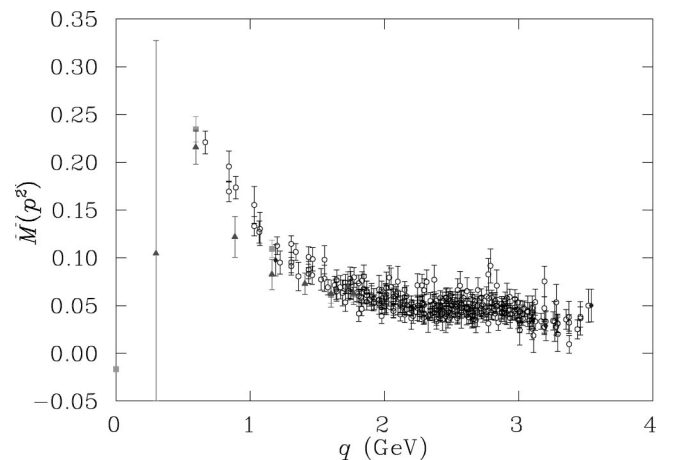


FIG. 7. Mass function for quark mass $ma=0.0125$ ($m \simeq 19$ MeV), Asqtad action in the ∂^2 (II) gauge. We see a lot of infrared noise at this low quark mass in this gauge. Compare with the Landau gauge result in Fig. 5 (bottom).

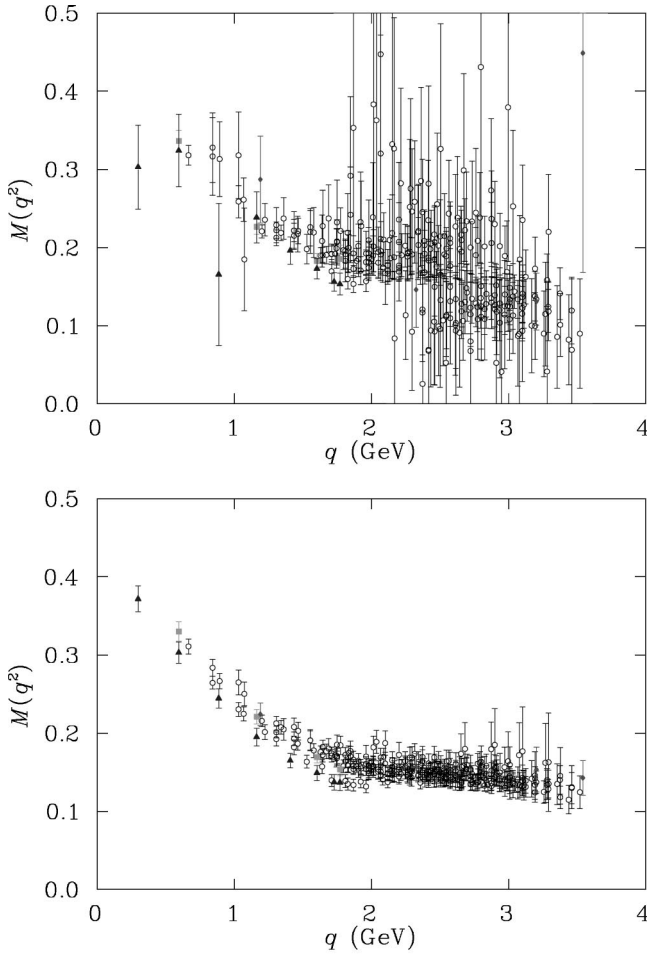


FIG. 8. The quark mass function with the Asqtad action in the $\partial^2(\text{III})$ gauge with $ma=0.05$. The upper data represents 76 configurations, some of which actually provide negative contributions. The signal is almost completely lost. The lower data represents 68 configurations. Removing the negative contributions has only barely restored the signal.

well. A fit to each of the mass functions was then done, using the ansatz

$$M(q) = \frac{c\Lambda^{1+2\alpha}}{q^{2\alpha} + \Lambda^{2\alpha}} + m_0, \quad (17)$$

which is a generalization of the one used in Ref. [4]. As we have seen, the quark mass function in the Laplacian gauge is almost indistinguishable from that in the Landau gauge, except that it is somewhat noisier (this may change at smaller lattice spacing). For this reason, we only show fits in the Landau gauge. Table I shows a sample of the fits. The table is divided into two sections, one in which the parameter α was held fixed and one in which it was allowed to vary. In the chiral limit we have used m_0 both as a fit parameter and by setting it to zero, although we show both results only for $\alpha=1.0$. When α is also allowed to vary, results for m_0 fixed and m_0 varying are in agreement, within errors. We see that for the heaviest mass, $\alpha=1.0$ provides an excellent fit, but in the chiral limit, $\alpha>1.0$ is somewhat favored. The role of α

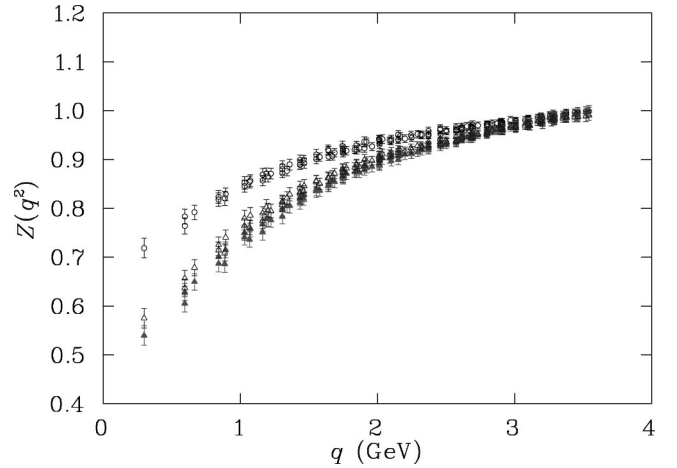


FIG. 9. Comparison of the quark Z functions for the Asqtad action for quark mass $ma=0.05$. Points marked with open circles are in Landau gauge, closed triangles are in $\partial^2(\text{I})$ gauge, and open triangles are in the $\partial^2(\text{II})$ gauge. The data have been cylinder cut.

may be seen in Fig. 14. At $\alpha=1.5$, the infrared and ultraviolet are significantly flatter, while the mass generation at around one GeV is made steeper.

For comparison, we also extrapolated, by linear fit, the fit parameters at each mass to zero mass. This is also reported in Table I, but we omit reporting any χ^2/dof . The linear fit was generally very good.

In this model, α is acting as a function of the bare mass, controlling the dynamical symmetry breaking. Unfortunately, the paucity of data points in the infrared leaves α poorly determined in the chiral limit. Furthermore, the degree to which our infrared data may be affected by the finite volume and by the chiral extrapolation is not really known. Finally, this ansatz is still crude in that it does not provide the correct asymptotic behavior.

As was explained in Sec. II, the quark mass function approaches the renormalized quark mass in the ultraviolet,

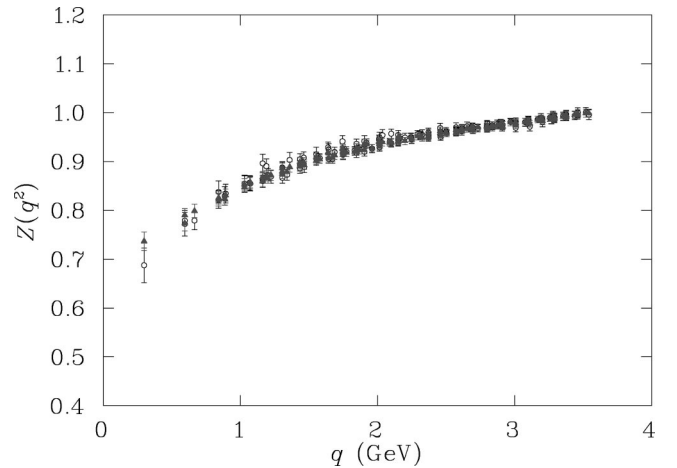


FIG. 10. Comparison of the Landau gauge quark Z functions for the heaviest ($ma=0.075$) and the lightest ($ma=0.0125$) quark masses, with the Asqtad action. The data have been cylinder cut. We see that over this range of values the mass dependence of the Z function is very weak.

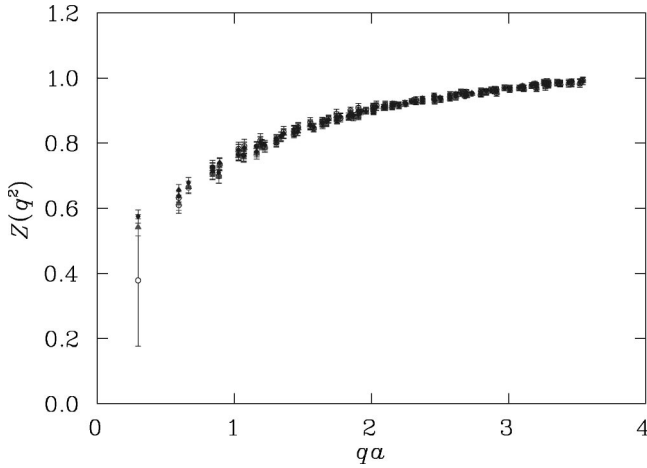


FIG. 11. Comparison of the quark Z functions for the three quark masses $ma=0.0125$, 0.025 , and 0.05 , with the Asqtad action in the $\partial^2(\text{II})$ gauge. Data have been cylinder cut. As in the Landau gauge, they agree to within errors, although there is a systematic ordering of the infrared points from heaviest quark (top) to lightest (bottom).

which itself becomes the bare mass in the $q \rightarrow \infty$ limit. It is a general feature of this study that the ultraviolet tail of $M(q)$ sits somewhat higher than the bare mass. The situation is summarized in Table II. This deviation from the correct asymptotic behavior is probably the consequence of an insufficiently small lattice spacing.

VII. CONCLUSIONS

We have seen that the Asqtad action provides a quark propagator with improved rotational symmetry compared to the standard Kogut-Susskind action and that the difference between them increases as we go to lighter quark masses. Furthermore, we have seen that the Asqtad action has smaller mass renormalization and better asymptotic behavior.

Our results for the quark propagator show that the quark

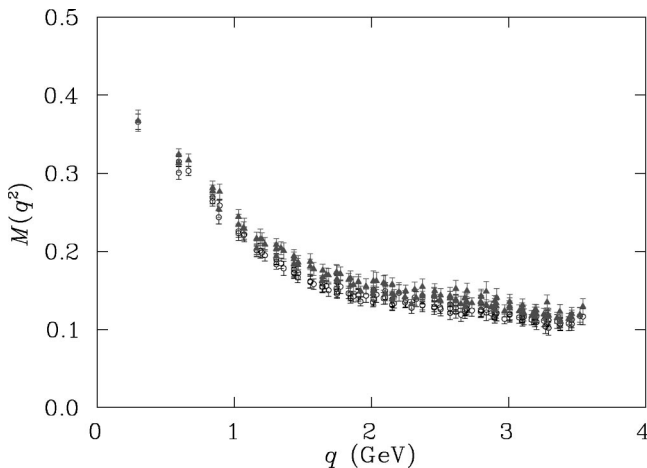


FIG. 12. Comparison of the quark mass functions for the Asqtad action, $ma=0.05$. Points marked with open circles are in the Landau gauge and closed triangles are in the $\partial^2(\text{I})$ gauge. Data have been cylinder cut.

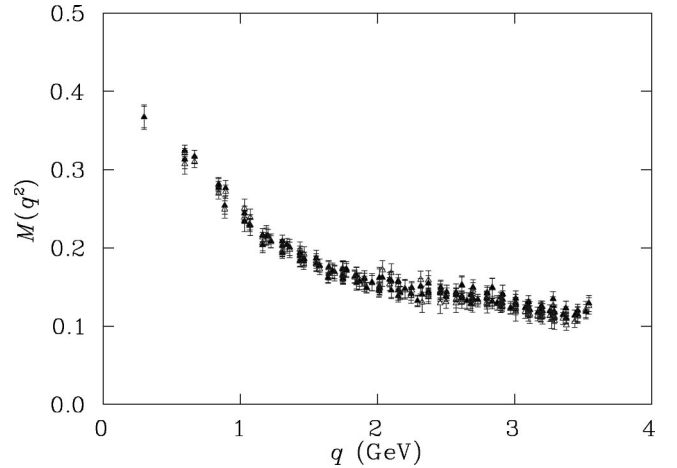


FIG. 13. Comparison of the quark mass functions for the Asqtad action, $ma=0.05$. Points marked with closed triangles are in the $\partial^2(\text{I})$ gauge and open triangles are in the $\partial^2(\text{II})$ gauge. Data have been cylinder cut.

mass function is the same, to within statistics in $\partial^2(\text{I})$ and $\partial^2(\text{II})$ gauges, while the Z function is slightly different. There is little difference between the quark mass function in the Landau gauge and in the Laplacian gauge, but the Z function dips more strongly in the infrared in the Laplacian gauge than in the Landau gauge. The infrared region of the Laplacian gauge mass function seems to be particularly badly af-

TABLE I. Best-fit parameters for the ansatz, Eq. (17), in the Landau gauge, in physical units. Where no errors are indicated, the parameter was fixed. Two different chiral extrapolations have been attempted: 1. The data was extrapolated to zero bare mass at each momentum, and then the ansatz was fit to the extrapolated data; 2. The fit parameters for each mass were extrapolated to zero mass. In the latter case, no χ^2/dof is reported. Errors are jackknife.

m (MeV)	c	Λ (MeV)	m_0 (MeV)	α	$M(0)$ (MeV)	χ^2 per dof
114	0.35(1)	910(20)	142(7)	1.0	462(9)	0.38
95	0.36(5)	880(70)	117(7)	1.0	440(20)	0.42
76	0.39(5)	830(70)	92(7)	1.0	420(20)	0.42
57	0.45(4)	770(50)	70(7)	1.0	410(20)	0.51
38	0.49(8)	720(60)	44(6)	1.0	400(30)	0.56
19	0.54(9)	670(60)	18(6)	1.0	380(30)	0.69
0	0.56(8)	650(50)	-12(6)	1.0	350(20)	0.66
0	0.80(20)	520(50)	0.0	1.0	400(40)	1.3
	0.55(10)	625(75)	-7(7)	1.0	340(20)	
114	0.28(1)	990(30)	155(7)	1.25(4)	428(7)	0.38
95	0.28(2)	965(40)	129(9)	1.30(10)	404(9)	0.37
76	0.30(2)	930(50)	105(7)	1.29(6)	380(10)	0.36
57	0.30(2)	910(40)	80(6)	1.30(2)	354(9)	0.41
38	0.36(4)	830(50)	54(7)	1.28(7)	350(20)	0.46
19	0.30(10)	800(200)	29(6)	1.4(3)	310(60)	0.55
0	0.30(4)	870(60)	0.0	1.52(23)	260(20)	0.49
	0.33(4)	810(60)	5(7)	1.46(4)	280(20)	

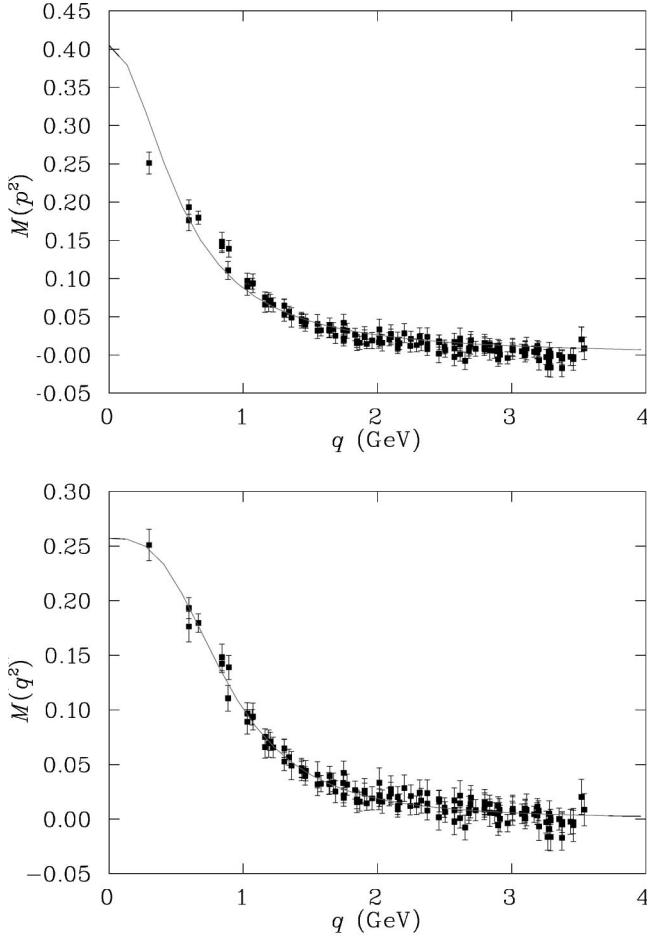


FIG. 14. Mass function extrapolated to the chiral limit. Errors are jack-knife. Fit parameters are top: $c=0.80(20)$, $\Lambda=520(50)$ MeV, $m_0=0.0$, $\alpha=1.0$, and $\chi^2/\text{dof}=1.3$, and bottom: $c=0.30(4)$, $\Lambda=870(60)$ MeV, $m_0=0.0$, $\alpha=1.52(23)$, and $\chi^2/\text{dof}=0.49$.

fectured by decreasing quark mass. We have seen that the $\partial^2(\text{III})$ gauge gives very poor results in $SU(3)$, in calculations of the quark propagator, consistent with results for the gluon propagator [11]. Overall the Landau gauge results of this work for the Asqtad appear to be consistent within errors with the results of earlier Landau gauge studies of the quark

TABLE II. Estimates of the Landau gauge quark mass function at zero four-momentum. Here m is the bare input mass and m_0 is the ultraviolet mass from the fit of the mass function.

$m(\text{MeV})$	$\alpha=1.0$		$\alpha \approx 1.3$	
	$M(0)(\text{MeV})$	m_0/m	$M(0)(\text{MeV})$	m_0/m
114	462(9)	1.25(6)	428(7)	1.35(6)
95	440(20)	1.23(7)	404(9)	1.36(6)
76	420(20)	1.21(9)	380(10)	1.38(9)
57	410(20)	1.2(1)	354(9)	1.4(1)
38	400(30)	1.16(16)	350(20)	1.4(2)
19	380(30)	1.0(3)	310(60)	1.5(3)

propagator [4–6]. Our results suggest that the M function is insensitive to whether we use the Landau or Laplacian gauge, whereas the Z function has an enhanced infrared dip in the Laplacian gauge.

As we have simulated on only one lattice, it remains to do a thorough examination of discretization and finite volume effects. The chiral limit was obtained by extrapolation, which may provide another source of systematic error. It will also be interesting to investigate the $\mathcal{O}(a^4)$ errors by using an improved gluon action. Further work may allow the development of a more sophisticated ansatz which has the correct asymptotic behavior. Finally, studies on finer lattices could be used to calculate the chiral condensate, light quark masses, and potentially Λ_{QCD} .

ACKNOWLEDGMENTS

The authors wish to thank Derek Leinweber and Jonivar Skullerud for useful discussions. The work of U.M.H. and P.O.B. was supported in part by DOE contract DE-FG02-97ER41022. The work of A.G.W. was supported by the Australian Research Council.

APPENDIX: STAGGERED QUARK PROPAGATORS

In this appendix we give the details of the quark propagator calculation using the Kogut-Susskind and Asqtad actions. The free KS action is

$$S = \frac{1}{2} \sum_{x,\mu} \bar{\chi}(x) \eta_\mu(x) (\chi(x+\mu) - \chi(x-\mu)) + m \sum_x \bar{\chi}(x) \chi(x), \quad (\text{A1})$$

where the staggered phases are $\eta_\mu(x) = (-1)^{\xi^{(\mu)} \cdot x}$ and

$$\xi_\nu^{(\mu)} = \begin{cases} 1 & \text{if } \nu < \mu, \\ 0 & \text{otherwise.} \end{cases} \quad (\text{A2})$$

To Fourier transform, write

$$k_\mu = \frac{2\pi n_\mu}{L_\mu} \Big|_{n_\mu} = 0, \dots, L_\mu - 1 \quad (\text{A3})$$

as $k_\mu = p_\mu + \pi \alpha_\mu$, where

$$p_\mu = \frac{2\pi m_\mu}{L_\mu} \Big|_{m_\mu} = 0, \dots, \frac{L_\mu}{2} - 1, \quad (\text{A4})$$

$$\alpha_\mu = 0, 1, \quad (\text{A5})$$

and define $\int_k \equiv \frac{1}{V} \sum_k$. Then

$$\int_k = \int_p \sum_{\alpha_\mu=0}^1, \quad (\text{A6})$$

$$\begin{aligned}\chi(x) &= \int_k e^{ik \cdot x} \chi(k) \\ &= \int_p \sum_{\alpha} e^{i(p + \pi\alpha) \cdot x} \chi_{\alpha}(p).\end{aligned}\quad (\text{A7})$$

Defining

$$\bar{\delta}_{\alpha\beta} = \Pi_{\mu} \delta_{\alpha\mu\beta} |_{\text{mod}2}, \quad (\text{A8})$$

$$(\bar{\gamma}_{\mu})_{\alpha\beta} = (-1)^{\alpha\mu} \bar{\delta}_{\alpha + \zeta^{(\mu)}, \beta}, \quad (\text{A9})$$

where the $\bar{\gamma}_{\mu}$ satisfy

$$\{\bar{\gamma}_{\mu}, \bar{\gamma}_{\nu}\} = 2 \delta_{\mu\nu} \bar{\delta}_{\alpha\beta}, \quad (\text{A10})$$

$$\bar{\gamma}_{\mu}^{\dagger} = \bar{\gamma}_{\mu}^T = \bar{\gamma}_{\mu}^{*} = \bar{\gamma}_{\mu}, \quad (\text{A11})$$

forming a ‘‘staggered’’ Dirac algebra. Putting all this together, we can derive a momentum space expression for the KS action,

$$S = \int_p \sum_{\alpha\beta} \bar{\chi}_{\alpha}(p) \left[i \sum_{\mu} (\bar{\gamma}_{\mu})_{\alpha\beta} \sin(p_{\mu}) + m \bar{\delta}_{\alpha\beta} \right] \chi_{\beta}(p). \quad (\text{A12})$$

From this we can see that, in momentum space, the tadpole improved, tree-level form of the quark propagator is

$$S_{\alpha\beta}^{-1}(p; m) = u_0 i \sum_{\mu} (\bar{\gamma}_{\mu})_{\alpha\beta} \sin(p_{\mu}) + m \bar{\delta}_{\alpha\beta}, \quad (\text{A13})$$

where p_{μ} is the discrete lattice momentum given by Eq. (A4). Assuming that the full propagator retains this form (in analogy to the continuum case) we write

$$S_{\alpha\beta}^{-1}(p) = i \sum_{\mu} (\bar{\gamma}_{\mu})_{\alpha\beta} \sin(p_{\mu}) A(p) + B(p) \bar{\delta}_{\alpha\beta} \quad (\text{A14})$$

$$= Z^{-1}(p) \left[i \sum_{\mu} (\bar{\gamma}_{\mu})_{\alpha\beta} \sin(p_{\mu}) + M(p) \bar{\delta}_{\alpha\beta} \right]. \quad (\text{A15})$$

For the KS action, it is convenient to define

$$q_{\mu} \equiv \sin(p_{\mu}) \quad (\text{A16})$$

as a shorthand.

Numerically, we calculate the quark propagator in coordinate space,

$$\begin{aligned}G(x, y) &= \langle \chi(x) \bar{\chi}(y) \rangle \\ &= \sum_{\alpha\beta} \int_{p, r} \exp\{i(p + \pi\alpha)x - i(r + \pi\beta)y\} \\ &\quad \times \langle \chi_{\alpha}(p) \bar{\chi}_{\beta}(r) \rangle \\ &= \sum_{\alpha\beta} \int_{p, r} \exp\{i(p + \pi\alpha)x - i(r + \pi\beta)y\} \\ &\quad \times \delta_{pr} S_{\alpha\beta}(p) \\ &= \sum_{\alpha\beta} \int_p \exp\{ip(x - y)\} \\ &\quad \times \exp\{i\pi(\alpha x - \beta y)\} S_{\alpha\beta}(p).\end{aligned}\quad (\text{A17})$$

To obtain the quark propagator in momentum space, we take the Fourier transform of $G(x, 0)$ and, decomposing the momenta as $k_{\mu} = r_{\mu} + \pi \delta_{\mu} |_{0 \leq r_{\mu} < \pi}$, get

$$\begin{aligned}G(k) &= G(r + \pi\delta) \equiv G_{\delta}(r) = \sum_x e^{-ikx} G(x, 0) \\ &= \sum_{\alpha\beta} \int_p \sum_x \exp\{-i(r + \pi\delta)x\} \\ &\quad \times \exp\{i(p + \pi\alpha)x\} S_{\alpha\beta}(p) \\ &= \sum_{\alpha\beta} \int_p \delta_{pr} \bar{\delta}_{\alpha\delta} S_{\alpha\beta}(p).\end{aligned}\quad (\text{A18})$$

Thus in terms of the KS momenta, q ,

$$G_{\delta}(q) = \sum_{\beta} S_{\delta\beta}(q) = Z(q) \frac{-i \sum_{\mu} (-1)^{\delta\mu} q_{\mu} + M(q)}{q^2 + M^2(q)}, \quad (\text{A19})$$

from which we obtain

$$\sum_{\delta} \text{Tr} G_{\delta}(q) = 16N_c \frac{Z(q)M(q)}{q^2 + M^2(q)} = 16N_c \mathcal{B}(q), \quad (\text{A20})$$

and

$$\begin{aligned}i \sum_{\delta} \sum_{\rho} (-1)^{\delta\rho} q_{\rho} \text{Tr} [G_{\delta}(q)] &= 16N_c q^2 \frac{Z(q)}{q^2 + M^2(q)} \\ &= 16N_c q^2 \mathcal{A}(q).\end{aligned}\quad (\text{A21})$$

Note: we could determine

$$A(p) = Z^{-1}(p) = \frac{-i}{16N_c \sum_{\nu} \sin^2(p_{\nu})} \times \sum_{\alpha\beta} \sum_{\rho} (\bar{\gamma}_{\rho})_{\alpha\beta} \sin(p_{\rho}) \text{Tr}[S_{\beta\alpha}^{-1}(p)], \quad (\text{A22})$$

$$B(p) = \frac{M(p)}{Z(p)} = \frac{1}{16N_c} \sum_{\alpha} \text{Tr}[S_{\alpha\alpha}^{-1}(p)], \quad (\text{A23})$$

but we would rather avoid inverting $S_{\alpha\beta}(p)$.

Putting it all together we get

$$A(q) = Z^{-1}(q) = \frac{\mathcal{A}(q)}{\mathcal{A}^2(q)q^2 + \mathcal{B}^2(q_{\mu})}, \quad (\text{A24})$$

$$B(q) = \frac{M(q)}{Z(q)} = \frac{\mathcal{B}(p)}{\mathcal{A}^2(q)q^2 + \mathcal{B}^2(p)}, \quad (\text{A25})$$

$$M(q) = \frac{\mathcal{B}(q)}{\mathcal{A}(q)}. \quad (\text{A26})$$

The tadpole improved, tree-level behavior of the Z and mass functions are simply

$$Z^0 = \frac{1}{u_0} \quad (\text{A27})$$

and

$$M^0 = \frac{m}{u_0}, \quad (\text{A28})$$

respectively.

The Asqtad quark action [3] is a fat-link Staggered action using three-link, five-link, and seven-link staples along with the three-link Naik term [16] and five-link Lepage term [17], with tadpole improved coefficients tuned to remove all tree-level $\mathcal{O}(a^2)$ errors. This action was motivated by the desire to minimize quark flavor changing interactions, but has also been reported to have good rotational symmetry.

At tree-level (i.e., no interactions, links set to the identity), the staples in this action make no contribution, so the action reduces to the Naik action:

$$S = \frac{1}{2} \sum_{x,\mu} \bar{\chi}(x) \eta_{\mu}(x) \left[\frac{9}{8} (\chi(x+\mu) - \chi(x-\mu)) - \frac{1}{24} (\chi(x+3\mu) - \chi(x-3\mu)) \right] + m \sum_x \bar{\chi}(x) \chi(x). \quad (\text{A29})$$

The quark propagator with this action has the tree-level form

$$S_{\alpha\beta}^{-1}(p;m) = u_0 i \sum_{\mu} (\bar{\gamma}_{\mu})_{\alpha\beta} \sin(p_{\mu}) \left[\frac{9}{8} \sin(p_{\mu}) - \frac{1}{24} \sin(3p_{\mu}) \right] + m \bar{\delta}_{\alpha\beta} \quad (\text{A30})$$

so we choose

$$q_{\mu}(p_{\mu}) \equiv \frac{9}{8} \sin(p_{\mu}) - \frac{1}{24} \sin(3p_{\mu}) \quad (\text{A31})$$

$$= \sin(p_{\mu}) \left[1 + \frac{1}{6} \sin^2(p_{\mu}) \right]. \quad (\text{A32})$$

Having identified the correct momentum for this action, we can calculate the invariant functions as before. No further tree-level correction is required.

-
- [1] S. Aoki *et al.*, Phys. Rev. Lett. **82**, 4392 (1999).
[2] D. Becirevic *et al.*, Phys. Rev. D **61**, 114507 (2000).
[3] K. Orginos, D. Toussaint, and R. L. Sugar, Phys. Rev. D **60**, 054503 (1999).
[4] J.-I. Skullerud and A. G. Williams, Phys. Rev. D **63**, 054508 (2001).
[5] J.-I. Skullerud, D. B. Leinweber, and A. G. Williams, Phys. Rev. D **64**, 074508 (2001).
[6] F. D. R. Bonnet, P. O. Bowman, D. B. Leinweber, A. G. Williams, and J. Zhang, Phys. Rev. D **65**, 114503 (2002).
[7] J. C. Vink and U.-J. Wiese, Phys. Lett. B **289**, 122 (1992).
[8] J. C. Vink, Phys. Rev. D **51**, 1292 (1995).
[9] C. Alexandrou, Ph. de Forcrand, and E. Follana, Phys. Rev. D **63**, 094504 (2001).
[10] C. Alexandrou, Ph. de Forcrand, and E. Follana, Phys. Rev. D **65**, 114508 (2002).
[11] P. O. Bowman, U. M. Heller, D. B. Leinweber, and A. G. Williams, hep-lat/0206010.
[12] Some of the numbers in this paper differ slightly from those published elsewhere [13] due to a revised value for the lattice spacing.
[13] P. O. Bowman, U. M. Heller, and A. G. Williams, Nucl. Phys. B (Proc. Suppl.) **106**, 820 (2002); **109**, 163 (2002).
[14] This is intended to be merely illustrative; in practice we never actually invert the propagator. See the Appendix for details.
[15] F. D. R. Bonnet, P. O. Bowman, D. B. Leinweber, A. G. Williams, and J. M. Zanotti, Phys. Rev. D **64**, 034501 (2001), and references contained therein.
[16] S. Naik, Nucl. Phys. **B316**, 238 (1989).
[17] G. P. Lepage, Phys. Rev. D **59**, 074502 (1999).
[18] C. T. H. Davies *et al.*, Phys. Rev. D **37**, 1581 (1988).